Since January 2020 Elsevier has created a COVID-19 resource centre with free information in English and Mandarin on the novel coronavirus COVID-19. The COVID-19 resource centre is hosted on Elsevier Connect, the company's public news and information website.

European Journal of Pharmacology 886 (2020) 173448

Contents lists available at ScienceDirect

European Journal of Pharmacology

journal homepage: www.elsevier.com/locate/ejphar

Full length article

In silico pharmacokinetic and molecular docking studies of natural flavonoids and synthetic indole chalcones against essential proteins of SARS-CoV-2

Balaji Gowrivel Vijayakumar [1], Deepthi Ramesh [1], Annu Joji, Jayadharini Jayachandra prakasan, Tharanikkarasu Kannan [*]

Department of Chemistry, Pondicherry University, Kalapet, Puducherry, 605014, India

ARTICLE INFO

Keywords:
Flavonoids
Indole chalcones
SARS-CoV-2
In silico
COVID-19
Phytochemicals

ABSTRACT

Severe acute respiratory syndrome coronavirus 2 (SARS-CoV-2) is distinctly infective and there is an ongoing effort to find a cure for this pandemic. Flavonoids exist in many diets as well as in traditional medicine, and their modern subset, indole-chalcones, are effective in fighting various diseases. Hence, these flavonoids and structurally similar indole chalcones derivatives were studied *in silico* for their pharmacokinetic properties including absorption, distribution, metabolism, excretion, toxicity (ADMET) and anti-SARS-CoV-2 properties against their proteins, namely, RNA dependent RNA polymerase (rdrp), main protease (M^{pro}) and Spike (S) protein via homology modelling and docking. Interactions were studied with respect to biology and function of SARS-CoV-2 proteins for activity. Functional/structural roles of amino acid residues of SARS-CoV-2 proteins and, the effect of flavonoid and indole chalcone interactions which may cause disease suppression are discussed. The results reveal that out of 23 natural flavonoids and 25 synthetic indole chalcones, 30 compounds are capable of M^{pro} deactivation as well as potentially lowering the efficiency of M^{pro} function. Cyanidin may inhibit RNA polymerase function and, Quercetin is found to block interaction sites on the viral spike. These results suggest flavonoids and their modern pharmaceutical cousins, indole chalcones are capable of fighting SARS-CoV-2. The *in vitro* anti-SARS-CoV-2 activity of these 30 compounds needs to be studied further for complete understanding and confirmation of their inhibitory potential.

1. Introduction

Coronavirus, the 21st-century pandemic highlights the role of viruses in emerging infectious diseases. It caused a vital onset of lethal pneumonia, initiated by the severe acute respiratory syndrome coronavirus (SARS-CoV) epidemic in 2003 (Rahman et al., 2020). The SARS-CoV-2 afflicted 213 countries around the world with more than 18 million infections and more than 0.7 million deaths worldwide as on August 5, 2020. The current global plight of COVID-19 is pandemic and the virus continues to sweep the world with no known cure. Coronaviruses are spherical positive RNA viruses in the *Coronaviridae* family with the largest genome amidst all RNA viruses (Weiss and Leibowitz, 2011; Wu et al., 2020a). The CoV genomes have non-structural proteins (nsps), replicase (RNA dependent RNA polymerase or rdrp) at 5′ end, open reading frames and structural proteins at 3′ end. The replication gene has two polyproteins (pp1ab and pp1a) for replication and transcription which are converted into 16 nsps by main protease (M^{pro}) (Jin et al., 2020b). These nsps produce subgenomic RNA encoding the structural proteins: spike (S), envelope (E), membrane (M) and nucleocapsid (N) proteins (Wu et al., 2020a). The N protein complexes with RNA forming the helical capsid in the viral envelope with other structural proteins embedded inside. The spike proteins projecting from the viral surface carries two domains (S1 and S2) and the receptor-binding domain (RBD) in S1 binds with angiotensin-converting enzyme 2 (ACE2) in host cells to mediate the integration of host and viral cells for viral entry (Ashour et al., 2020; Cui et al., 2019). This initiates replication and once inside the host cell, rdrp produces viral mRNA or messenger RNA from template RNA which undergoes translation forming non-structural and

* Corresponding author.
E-mail addresses: vgbalaji91@gmail.com (B.G. Vijayakumar), naksha.deepz92@gmail.com (D. Ramesh), annujoji@gmail.com (A. Joji), dharinijcprakash@gmail.com (J. Jayachandra prakasan), tharani.che@pondiuni.edu.in (T. Kannan).
[1] Indicates equal contribution.

https://doi.org/10.1016/j.ejphar.2020.173448
Received 10 June 2020; Received in revised form 29 July 2020; Accepted 29 July 2020
Available online 6 August 2020

structural proteins. The process is error-laden as rdrp lack proofreading functions, increasing the mutation rate within the virus (Venkataraman et al., 2018).

The present-day SARS-CoV-2 has 89% nucleotide similarity and 80% identity with SARS-CoV (Wu et al., 2020b). When correlated with Middle East respiratory syndrome coronavirus (MERS-CoV) and SARS-CoV, current SARS-CoV-2 shows 96% sequence identity with a bat CoV, RaTG13, indicating a common ancestral origin (Guo et al., 2020; Zhou et al., 2020). Despite endeavours to develop a cure after MERS and SARS coronaviruses, vaccines or drugs are still lacking. The antivirals used currently reduce transmission and give symptomatic relief. Current approaches toward anti-corona agents include repurposing of drugs, screening of promising molecules using an extant database or developing a novel vaccine using genomic information of CoVs (Wu et al., 2020a). The main drug targets for CoV include the M^{pro}, rdrp and spike proteins. An *in-silico* approach of screening existing database to find a variety of compounds inhibiting coronavirus against these targets can save time by filtering out candidates worthy of *in vitro* analysis.

One such set of compounds are flavonoids given in Table 1 ubiquitous in vegetables, fruits, herbs and in traditional medicines (He et al., 2018; Li et al., 2016; Xu et al., 2013). Flavonoids exhibit antiviral (Dai et al., 2019), antibacterial (Yixi et al., 2015), antimicrobial (Cushnie and Lamb, 2005), anticancer (Chahar et al., 2011), antidiabetic (AL-Ishaq et al., 2019), anti-inflammatory (He et al., 2018) and antifungal (Weidenbörner et al., 1990) properties. Recent reports show quercetin based antiviral drug Gene-Eden-VIR/Novirin inhibiting the protease of SARS-CoV-2 (Polansky and Lori, 2020). Chalcones in flavonoids subset inhibit tobacco mosaic virus (Tang et al., 2019), HIV (Wu et al., 2003), herpes (Hassan et al., 2015) and dengue virus (Kiat et al., 2006) along with antioxidant (Biradar et al., 2010), antimicrobial (Burmaoglu et al., 2017), antimycobacterial (Chiaradia et al., 2012) and antileishmanial (de Mello et al., 2018) properties. The alkylated chalcones extracted from *Angelica keiskei* inhibit SARS-CoV protease (Park et al., 2016).

In this study, we have taken 23 natural flavonoids and 25 anti-tubercularly active synthetic indole chalcones (Ramesh et al., 2020) and studied *in silico* for their potential anti-SARS-CoV-2 activity along with their physicochemical and absorption, distribution, metabolism, excretion, toxicity (ADMET) properties.

2. Materials and methods

The molinspiration (2002) and pkCSM (Pires et al., 2015) servers were used to analyse the pharmacokinetic properties of flavonoids. The crystal structures of proteins were acquired from the RCSB Protein Data Bank (PDB) based on resolution and R factors specifically 6M71, 6YB7, and 6LZG. Homology modelling of selected proteins of SARS-CoV-2 was performed using online server SWISS-MODEL (Schwede et al., 2003). The quality of the protein structures was appraised by the Ramachandran plot (Lovell et al., 2003) using PROCHECK (Laskowski et al., 1993) webserver. The proteins were made ready using AutoDock Tools v.1.5.6. to remove unwanted co-crystallized molecules, to add charges (Gaussian, Gasteiger), and to incorporate polar hydrogens. Their energy minimized ligand data was developed on PerkinElmer Chem3D v15.0. Blind docking was achieved using AutoDock Vina v.1.1.2 (Trott and Olson, 2010) and PyRx-Python Prescription v0.8 (Dallakyan and Olson, 2015) to assist. Binding affinity for poses with RMSD lower than 2 Å was noted in kcal/mol. Post-docking analysis of protein-ligand interactions was conducted on BIOVIA Discovery Studio Visualizer v.19.1.0. (2018). The synthesis and characterization of indole chalcones were published already by us and the synthetic procedure is available in the literature (Ramesh et al., 2020).

Table 1
Biological activities of natural flavonoids.

Name	Compound CID	Bioactivity	Reference
Luteolin	5280445	Inhibition of Japanese encephalitis virus	Fan et al. (2016)
Apigenin	5280443	Inhibition of Foot-and-mouth disease virus (FMDV) and Enterovirus-71 infection	(Qian et al., 2015; Zhang et al., 2014)
Tangeritin	68077	Inhibition of respiratory syncytial virus (RSV)	Xu et al. (2014)
Kaempferol	5280863	Inhibition of influenza virus	Dong et al. (2014)
Quercetin	5280343	Inhibition of dengue and influenza virus	(Wu et al., 2015; Zandi et al., 2011)
Myricetin	5281672	Inhibition of tobacco mosaic virus and anti-HIV activity	(Semwal et al., 2016; Tang et al., 2020)
Fisetin	5281614	Inhibition of enterovirus-A71	(Lalani and Poh, 2020; Lin et al., 2012)
Hesperitin	72281	Inhibition of influenza virus	Dong et al. (2014)
Naringenin	932	Inhibition of dengue virus	(Frabasile et al., 2017; Salehi et al., 2019)
Eriodictyol	440735	Anti-diabetic, anti-inflammatory and anti-osteoclastogenic agent	(Wang et al., 2018; Zhang et al., 2012)
Liquiritin	503737	Anti-inflammatory, antiviral and anti-microbial	(Chirumbolo, 2016; Yu et al., 2015)
Genistein	5280961	Inhibition of African swine flu virus and herpes virus	(Andres et al., 2009; Arabyan et al., 2018; LeCher et al., 2019)
Daidzein	5281708	Inhibition of herpes virus	Argenta et al. (2015)
Calophyllolide	5281392	Anti-HIV activity	Liu et al. (2015)
Cyanidin	128861	Anti-HIV activity	(Kannan and Kolandaivel, 2018; Kaur et al., 2020)
Delphinidin	68245	Inhibition of flavivirus, zika virus and dengue virus	Vázquez-Calvo et al. (2017)
Malvidin	159287	Anti-HIV and anti-RSV	Mohammadi Pour et al. (2019)
Pelargonidin	440832	Anti-HIV and anti-RSV	Mohammadi Pour et al. (2019)
Peonidin	441773	Anti-HIV and anti-RSV	Mohammadi Pour et al. (2019)
Phloridzin	6072	Antiviral, anticancer and cardioprotective agents	Gupte and Buolamwini (2009)
Arbutin	440936	Anti-inflammatory and antioxidant agent	Migas and Krauze-Baranowska (2015)
Phloretin	4788	Inhibition of zika virus	Lin et al. (2019)
Chalconaringenin	5280960	Immunomodulation, anti-inflammatory, antiviral, anticancer, and antimicrobial properties	Lee et al. (2015)

3. Results

3.1. Pharmacokinetic investigation of flavonoids

Pharmacokinetic properties are an elemental segment of drug development to identify the biological properties of drug candidates. Lipinski's rule of five (Lipinski et al., 1997) and Veber's rules (Veber et al., 2002) were used to check the drug-likeness. Flavonoids given in

Table 1 were analysed for their physicochemical properties and the results are epitomized in Table 2. The ADMET characteristics of the flavonoids were studied to understand their pharmacokinetic profile and the results are given in Table 3.

3.2. Homology of SARS-CoV-2 proteins

The SARS-CoV-2 proteins, namely RNA dependent RNA polymerase (PDB: 6M71), M^{pro} (PDB: 6YB7) and Spike protein (PDB: 6LZG) showed 96.348%, 96.078% and 72.778% sequence identity with rdrp NSP12 (PDB: 6NUR), main protease (PDB: 2Z9J) and spike protein (PDB: 2AJF) respectively with SARS-CoV. The data indicated that 98.9% (M^{pro}, PDB: 6YB7), 99.4% (spike protein, PDB: 6LZG) and 99.9% (rdrp, PDB: 6M71) residues are in Ramachandran favoured regions. The Ramachandran plots for each protein are given in supplementary data.

3.3. Protein-ligand docking studies

Analysis of protein-ligand docking revealed the following: Cyanidin binds at ASP761 catalytic residue on rdrp. Compounds C25, Daidzein, Eriodictyol, Fisetin, Genistein, Kaempferol, Myricetin, Quercetin, Arbutin, Chalconaringenin, Phloretin and Liquiritin interact on the spike proteins' key RBD. Out of 48 compounds, 45 compounds from the library interact with M^{pro} at important residues. The comprehensive list of drugs, their binding affinity and amino acid interactions can be found in the supplementary material in Fig. S1 and Table S2 respectively. The important results are discussed in detail in the subsequent sections.

4. Discussion

4.1. Pharmacokinetic investigation of flavonoids

Out of 23 natural flavonoids listed in Fig. 1, nineteen flavonoids are showing no violation of the Lipinski's and Veber's rules and hence display druglike molecular (DLM) nature. The Log P values of 22 flavonoids are within the range of −1.36 to 3.78, while Calophyllolide shows one violation with a higher Log P value of 6.63. Molecular weight and number of H-acceptors of all flavonoids are within the accepted values of less than 500 and 10 respectively. Myricetin, Delphinidin, Phloridzin and Arbutin show violation in the number of H-bond donors. However, all the flavonoids are following the criteria of Veber's rules with total polar surface area (TPSA) values and the count of rotatable bonds within range for oral availability. The indole chalcones given in Fig. 2 are also obeying the aforementioned rules and show excellent DLM properties (Ramesh et al., 2020).

The parameters for evaluating the drug absorption was solubility and Caco-2 permeability as listed in Table 3. The solubility ranges from −6 to −2 indicating the moderate to the high solubility of flavonoids. The high water solubility can be due to 2–6 hydroxy groups present in each compound capable of forming bonds with water molecules. The human colonic adenocarcinoma cell line Caco-2 permeability of 10 compounds are high while myricetin, liquiritin, phloridzin, arbutin, phloretin, and chalconaringenin show poor permeation. The gastrointestinal absorption of the flavonoids is high except for phloridzin, arbutin and liquiritin which only show 40% absorption rate. The low absorption rate of compounds is a direct effect of its molecular size. However, an exception is Calophyllolide showing intestinal absorption of 97% despite its high molecular weight. The distribution of drug candidates considers the volume of distribution (VDss), blood-brain barrier (BBB) permeability, fraction unbound and central nervous system (CNS) permeability. The Log VDss values of less than 0.45 indicate the higher distribution of these drugs in plasma than in the tissues, except for Calophyllolide showing Log VDss vslue of <0.53. The fraction bound indicates the efficacy with which the compounds can diffuse. The compounds are not BBB permeant as none of the flavonoids has Log BBB >0.3. In the case of CNS penetration, 15 flavonoids have Log P values from −3 to −2 range, indicating moderate to high permeability. The ability to penetrate CNS is significant as there are reports of coronavirus targeting the CNS, owing to the presence of angiotensin-converting enzyme 2 receptors in neurons and glial cells (Baig et al., 2020). The metabolism and total clearance of the flavonoids were analysed. The flavonoids showed no hepatotoxicity, while 5 compounds showed Ames toxicity and hence may be mutagenic. In a collective sense, the ADMET profile of the flavonoids is satisfactory and hence suitable for *in silico* studies with SARS-CoV-2 proteins.

Table 2
Physicochemical properties of flavonoids under study.

Name	Lipinski's Rule of 5					Veber's Rule	
	Log P	Mole. Wt.	Hydrogen donor	Hydrogen acceptor	No. of violations	Total polar surface area (Å^2)	No. of rotatable bonds
Luteolin	1.97	286.24	4	6	0	111.12	1
Apigenin	2.46	270.24	3	5	0	90.89	1
Tangeritin	3.78	372.37	0	7	0	76.38	6
Kaempferol	2.17	286.24	4	6	0	111.12	1
Quercetin	1.68	302.24	5	7	0	131.35	1
Myricetin	1.39	318.24	6	8	1	151.58	1
Fisetin	1.97	286.24	4	6	0	111.12	1
Hesperitin	1.99	316.26	4	7	0	120.36	2
Naringenin	2.46	270.24	3	5	0	90.89	1
Eriodictyol	1.97	286.24	4	6	0	111.12	1
Liquiritin	0.41	418.40	5	9	0	145.91	4
Genistein	2.27	270.24	3	5	0	90.89	1
Daidzein	2.56	254.24	2	4	0	70.67	1
Calophyllolide	6.63	414.50	0	4	1	48.68	4
Cyanidin	−0.75	287.25	5	6	0	112.31	1
Delphinidin	−1.04	303.25	6	7	1	132.54	1
Malvidin	−0.42	331.30	4	7	0	110.55	3
Pelargonidin	−0.26	271.25	4	5	0	92.08	1
Peonidin	−0.44	301.27	4	6	0	101.32	2
Phloridzin	0.40	436.41	7	10	1	177.13	7
Arbutin	−1.36	288.25	6	8	1	139.84	3
Phloretin	2.66	274.27	4	5	0	97.98	4
Chalconaringenin	2.69	272.26	4	5	0	97.98	3

Note: Pharmacokinetic properties are analysed using the Molinspiration server (http://www.molinspiration.com).

Table 3
ADMET properties of flavonoids.

Name	Absorption			Distribution				Metabolism	Excretion	Toxicity	
	Solubility Log S (log mol/L)	Caco-2 perm. (log Papp in 10^{-6} cm/s)	Intestinal. absorption. (% Abs)	VDss (log L/kg)	Fraction. Unbound (Fu)	BBB perm. (log BB)	CNS perm. (log PS)		Total clearance (log ml/min/kg)	Hepato toxicity	Ames toxicity
Luteolin	−3.019	0.649	78.93	0.065	0.11	−1.185	−2.42	CYP1A2, CYP3A4 inhibitor	0.62	No	No
Apigenin	−2.77	1.034	90.842	0.007	0.198	−0.908	−2.168	CYP1A2, CYP2C19, CYP2C9 inhibitor	0.661	No	No
Tangeritin	−4.379	1.429	99.904	−0.326	0.088	−0.942	−2.958	CYP3A4 substrate, CYP1A2, CYP2C19, CYP2C9 inhibitor	0.862	No	No
Kaempferol	−3.191	0.879	82.139	0.234	0.125	−1.189	−2.36	CYP1A2, CYP2C9 inhibitor	0.649	No	Yes
Quercetin	−3.262	0.737	69.799	0.361	0.067	−1.453	−3.403	CYP1A2 inhibitor	0.608	No	No
Myricetin	−3.03	0.357	55.482	0.333	0.097	−1.797	−3.727	CYP1A2 inhibitor	0.598	No	No
Fisetin	−3.155	0.777	80.112	0.2	0.094	−1.175	−2.382	CYP1A2, CYP2C9, CYP3A4 inhibitor	0.573	No	No
Hesperitin	−3.34	1.145	74.297	0.448	0.087	−1.369	−3.314	CYP1A2, CYP2C9 inhibitor,	0.698	No	Yes
Naringenin	−2.77	1.034	90.842	0.007	0.198	−0.908	−2.168	CYP1A2, CYP2C19, CYP2C9 inhibitor	0.661	No	No
Eriodictyol	−3.019	0.649	78.93	0.065	0.11	−1.185	−2.42	CYP1A2, CYP3A4 inhibitor	0.62	No	No
Liquiritin	−3.681	−0.164	45.76	−0.431	0.198	−1.419	−4.001	No	0.482	No	Yes
Genistein	−2.945	0.942	91.714	−0.029	0.154	−0.9	−2.187	CYP1A2, CYP2C19, CYP2C9 inhibitor	0.297	No	No
Daidzein	−3.531	0.949	93.327	−0.136	0.221	−0.177	−1.971	CYP1A2, CYP2C19, CYP2C9, CYP2D6 inhibitor	0.203	No	Yes
Calophyllolide	−6.575	0.989	97.623	0.53	0.115	−0.398	−1.44	CYP3A4 substrate, CYP1A2, CYP2C19, CYP2C9 inhibitor	0.868	No	No
Cyanidin	−3.192	0.799	78.013	0.304	0.05	−1.395	−2.354	CYP1A2 inhibitor	0.787	No	No
Delphinidin	−3.003	0.707	65.867	0.227	0.073	−1.747	−3.545	CYP1A2 inhibitor	0.802	No	No
Malvidin	−3.654	1.042	74.828	0.343	0.048	−1.429	−3.244	CYP1A2, CYP2C9 inhibitor	0.927	No	No
Pelargonidin	−3.148	0.957	88.181	0.284	0.111	−1.124	−2.096	CYP1A2, CYP2C19, CYP2C9, CYP3A4 inhibitor	0.803	No	No
Peonidin	−3.398	0.996	82.489	0.342	0.066	−1.307	−2.264	CYP1A2, CYP2C19, CYP3A4 inhibitor	0.857	No	No
Phloridzin	−3.507	0.051	41.007	0.167	0.156	−1.751	−4.315	No	0.801	No	Yes
Arbutin	−2.189	0.27	41.21	−0.184	0.425	−1.416	−4.745	No	0.722	No	No
Phloretin	−2.885	0.349	70.9	−0.361	0.208	−1.261	−2.734	CYP1A2, CYP2C9,	0.263	No	No

(*continued on next page*)

Table 3 (*continued*)

Name	Absorption			Distribution				Metabolism	Excretion	Toxicity	
	Solubility Log S (log mol/L)	Caco-2 perm. (log Papp in 10^{-6} cm/s)	Intestinal. absorption. (% Abs)	VDss (log L/kg)	Fraction. Unbound (Fu)	BBB perm. (log BB)	CNS perm. (log PS)		Total clearance (log ml/min/kg)	Hepato toxicity	Ames toxicity
Chalconaringenin	−2.874	0.407	71.479	−0.408	0.202	−1.242	−2.618	CYP3A4 inhibitor CYP1A2, CYP2C9, CYP3A4 inhibitor	0.163	No	No

CYP: Cytochrome, BBB: Blood brain barrier, VDss: volume of distribution, perm.: permeability.

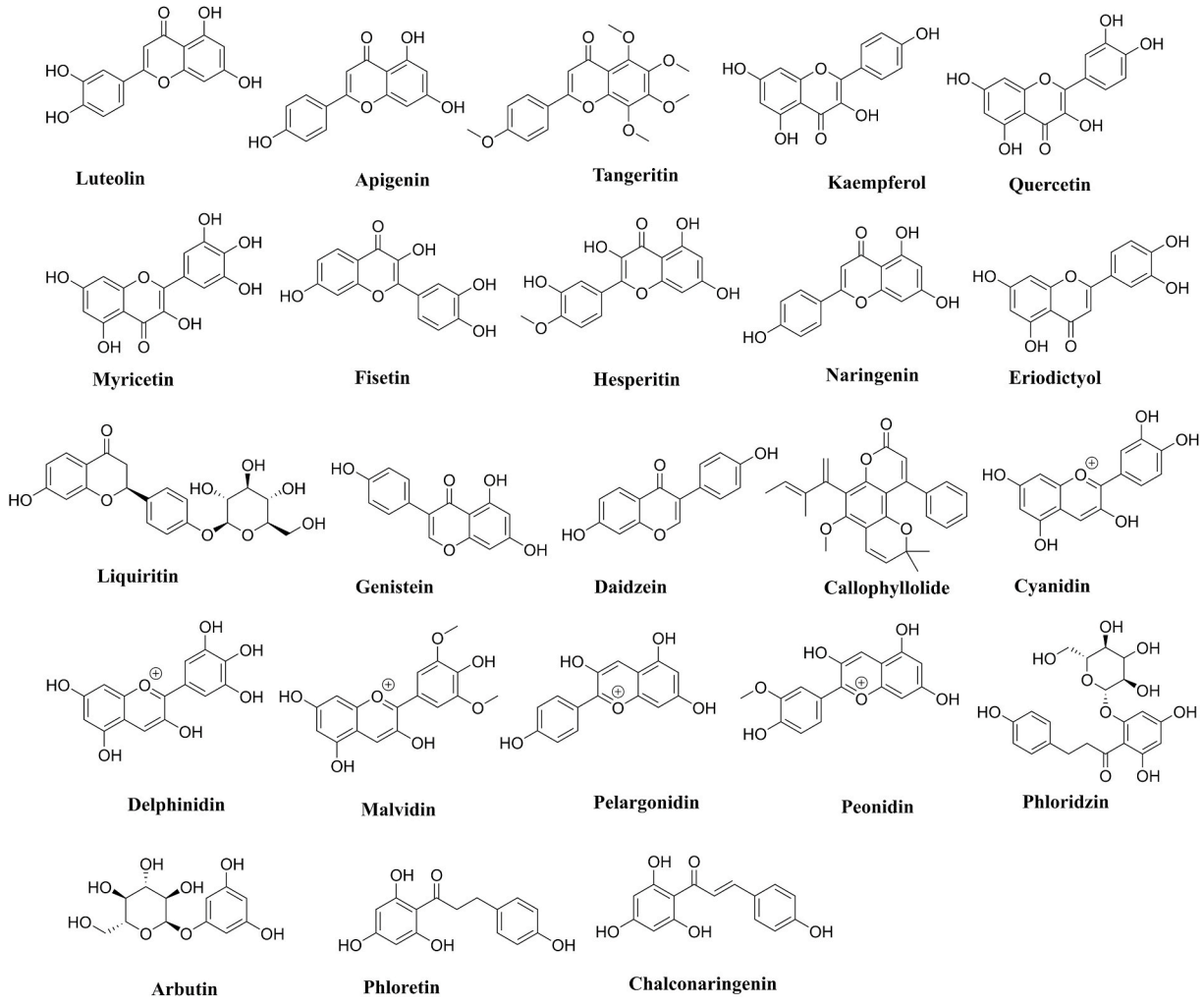

Fig. 1. Natural flavonoids used in the current study.

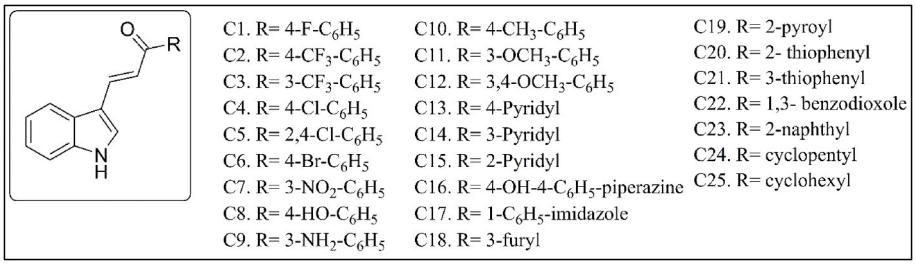

Fig. 2. Synthetic indole chalcones used in the current study.

4.2. Homology of SARS-CoV-2 proteins and protein-ligand docking studies

Homology modelling revealed that the M^{pro}, rdrp and Spike proteins of SARS-CoV-2 are remarkably similar to SARS-CoV in sequence, and their quality based on the Ramachandran plots was adequate for docking study. The anti-coronavirus drug design strategy can be classified based on different pathways of action. These can be the inhibition of proteins like M^{pro} or enzymes which are required for viral RNA replication and synthesis (rdrp) or, the inhibition of structural proteins like spike protein for adhering to host cells by inhibiting the spike – angiotensin-converting enzyme 2 domain. Interactions between the docked ligands and proteins predict possible modes of action or lack thereof. The compounds with lower binding energy can have a higher affinity towards target proteins. The following sections cover significant docking results and analysis.

4.2.1. RNA dependent RNA polymerase (rdrp)

The replication mechanism of SARS-CoV-2 is chiefly led by rdrp, a complex of nsp12, nsp8 and nsp7 (Jacome et al., 2015; Tan et al., 2018). The structure resembles a partially curled right hand grip and can be assorted into three regions namely the palm, the thumb and the fingers (Gao et al., 2020). This rdrp protein (PDB: 6M71) is largely carried over from SARS-CoV and provides certain targets of opportunity (Elfiky, 2020; Gao et al., 2020; Yin et al., 2020) for the selected flavonoids. The key catalytic residue sequence of Ser759, Asp760, and Asp761 on the palm region is the binding site of RNA; assisted in part by Asp618 which is the divalent cation binding residue, these are essential to the replication (Elfiky, 2020; Gao et al., 2020; Yin et al., 2020). Residues, Lys545 and Arg555 stabilize the incoming orientation of RNA while Lys500 and Ser501 mobilize to accommodate its approach (Yin et al., 2020). In addition to these residues, 29–50 on β-hairpin of nsp12 are held responsible for rdrp structural stabilization by interacting with other domains of nsp12 (Yin et al., 2020).

Post docking analysis shows that library members C4, C8, C12, C16, C17, C20, C22, C23, Calophyllolide, Genistein, Quercetin, Tangeritin, Arbutin and Liquiritin interact with β-hairpin residues (29–50). Unfortunately, literature to predict the outcome of these particular β-hairpin interactions in terms of rdrp function or stability is insufficient at present. However, it was encouraging to note that Cyanidin shows H-bonding with Asp761 (as shown in Fig. 3) at the RNA binding site with a binding affinity of −7.7 kcal/mol, suggesting that it may hinder the replication mechanism (Yin et al., 2020).

4.2.2. Main protease (M^{pro})

Viral RNA is translated into various polyproteins by the action of the main protease (M^{pro}) in SARS-CoV-2 (PDB: 6YB7) (Anand et al., 2003; Zhang et al., 2020b). The human equivalent for this particular protease is absent, thus, this is a safe target for anti-SARS-CoV-2 agents. The M^{pro}, in active form is a dimer of identical protomers (Neuman et al., 2011; Yang et al., 2003; Zhang et al., 2020b). Each protomer has 3 domains with the region between I and II being the main site of catalysis between residues, Cys145 and His41, while, the cleft between domains II and III is reserved for protomer dimerization (Shi and Song, 2006; Zhang et al., 2020b). The main catalytic site is shaped by the dimerization process which involves the residues between domains II and III (Jin et al., 2020a; Wei et al., 2006; Yang et al., 2003). Residues Met6, ARG4, Glu290, and Arg298 are responsible for this monomer-dimer behavior (Wei et al., 2006; Zhang et al., 2020b). Removal/mutation of these amino acids has shown the loss of M^{pro} activation and reversion to protomer form (Shi et al., 2008; Yang et al., 2003). Catalytic efficiency is regulated by residues 284–286 (Zhang et al., 2020b), special emphasis on Ala285 (Shi and Song, 2006) which is credited with making M^{pro} in SARS-CoV-2 several times more effective than its predecessor, SARS-CoV (Wei et al., 2006). Mutation at Glu288 and Asp289 was also held responsible for disruption of M^{pro} and certain other amino acids such as Lys5 interact with one or more of the aforementioned in a support capacity (Shi et al., 2008). Post docking analysis was astounding as with the exceptions of Arbutin and Calophyllolide almost all the candidates show some form of desirable interaction. Forty compounds at protease regulatory sites and 30 at critical junctures are responsible for activation/shaping of the catalytic site, with 22 compounds common to both categories as shown in Fig. 4.

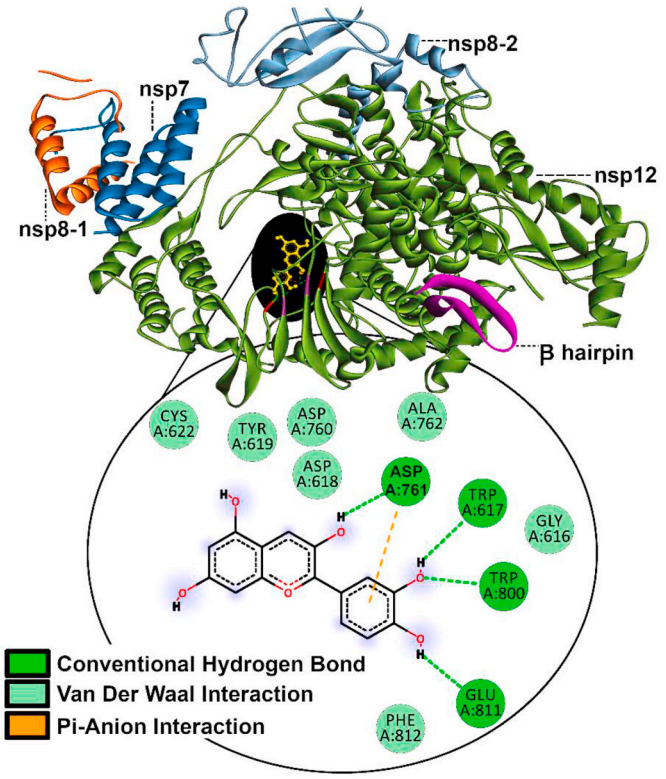

Fig. 3. Binding mode of Cyanidin to rdrp.

The key sites included are Glu288, Asp289, Glu290, and Lys5 whereas Ala285 and Leu286 are the regulatory sites of interaction. Except for C16 from indole chalcones and 7 flavonoids (Calophyllolide, Daidzein, Luteolin, Peonidin, Tangeritin, Arbutin and Phloridzin), all compounds interact with Leu286. The chalcones, C3 and C12 also interacted with Ala285. Overall, the flavonoids are more favourable with a maximum of three key residue interactions, whereas the indole chalcones are limited to a maximum of two. The best candidates were C23 indole-chalcone with a binding affinity of −10.4 kcal/mol interacting at Glu288, Asp289 and, the flavonoid Quercetin with an additional Glu290 interaction at −9.2 kcal/mol as given in Fig. 5.

4.2.3. Spike (S) protein

An appealing SARS-CoV-2 target is a spike (S) protein, which attacks the human angiotensin converting enzyme 2 receptors (South et al., 2020; Wang et al., 2016, 2020; Zhang et al., 2020a). Recent studies show us the spike protein is split into subunits S1 and S2 by the host proteases; S1 is made up of two domains one C-terminal (CTD) and an N-terminal (NTD) (Wang et al., 2020). The CTD is used by SARS-CoV-2 to bind to, and, it is further divided into external and core subdomains (Wang et al., 2020). This CTD external subdomain is made up of two β-strands attached to a flexible loop and, is primarily responsible for receptor recognition and binding (Wang et al., 2020). Some of the residues that the external subdomain of SARS-CoV-2 S1 CTD uses to bind to the receptor include, Tyr453, Gly496, Gln498, Asn501, Gly502, Tyr503, and Tyr505 (Wang et al., 2020).

These residues are pertinent as seen from the post-docking analysis of compounds. The compounds, C25, Daidzein, Eriodictyol, Fisetin,

Activation or Dimerisation sites

Glu288, Asp289, Glu290
Apigenin, Cyanidin, Daidzein, Myricetin, Quercetin

Glu290, Asp289, Lys5
Hesperitin, Peonidin, Phloridzin

Glu288, Asp289
C9, C12, C14, C15, C17, C19, C23, Kaempferol, Luteolin, Naringenin, Pelargonidin, Chalconaringenin

Asp289
C3, C6, C16, Fisetin, Genistein, Tangeritin, Liquiritin

Regulatory sites

Ala285
C3, C12

Leu286
C1, C2, C3, C4, C5, C6, C7, C8, C9, C10, C11, C12, C13, C14, C15, C17, C18, C19, C20, C21, C22, C23, C24, C25, Apigenin, Kaempferol, Quercetin, Myricetin, Fisetin, Hesperitin, Naringenin, Eriodictyol, Liquiritin, Genistein, Cyanidin, Delphinidin, Malvidin, Pelargonidin, Phloretin, Chalconaringenin

Note: Red highlights compounds having interactions in both activation/dimerisation and regulatory sites

Fig. 4. Sites of compound interaction on M^{pro}.

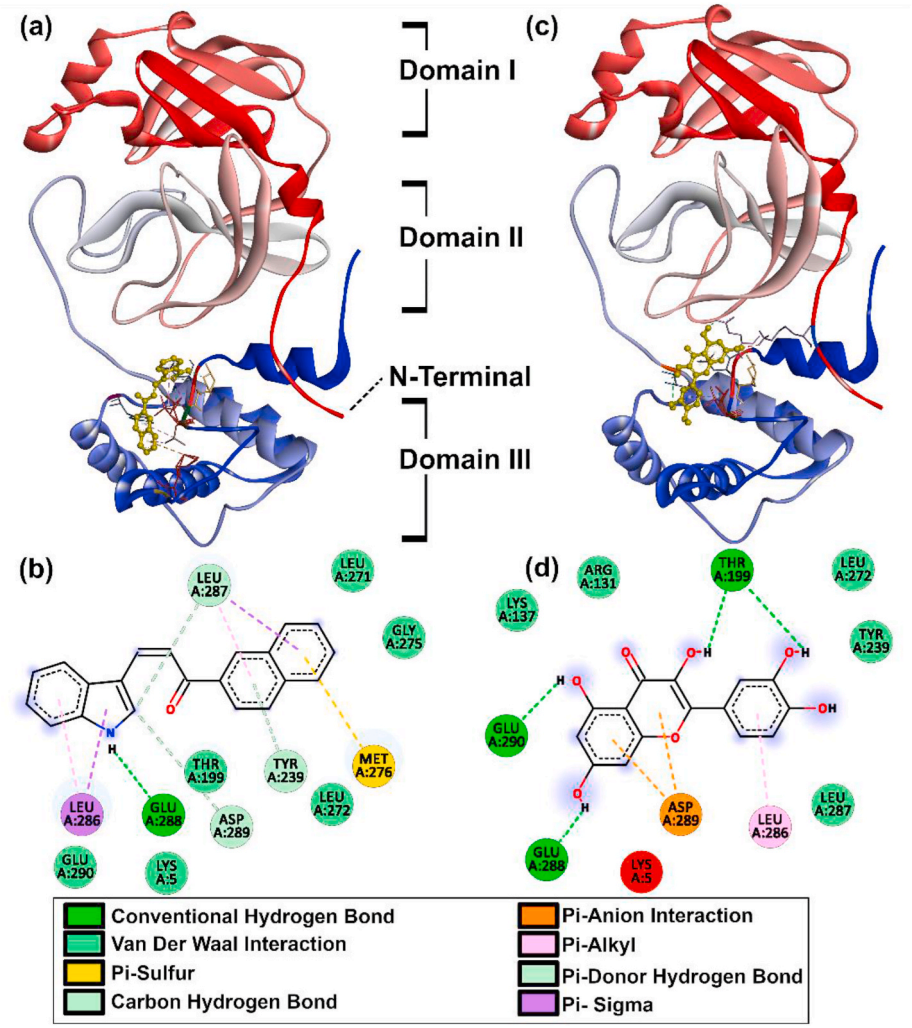

Fig. 5. Binding mode of Mpro with (a) C23 in 3D (b) C23 in 2D with amino acid interactions (c) Quercetin in 3D (d) Quercetin in 2D with amino acid interactions.

Genistein, Kaempferol, Myricetin, Quercetin, Arbutin, Chalconaringenin, Phloretin and Liquiritin, evidently all have one or more interactions with these residues. C17 and Luteolin have some minor interaction with residues Asn450 and Arg457 which are adjacent to key sites Tyr449 and Phe456 respectively (Wang et al., 2020). Quercetin proved superior as it was most tightly bound with a −7.8 kcal/mol binding affinity at Gly496, Asn501, Tyr505 and Tyr453 residues as shown in Fig. 6. These compounds, by occupying specific residues may show some effect in thwarting the spike protein's ability to bind and, warrant further study (*in vitro)* of flavonoids as competitive inhibitors of the spike protein.

4.3. Structure-activity relationships (SARs)

The SARs of the compounds is derived from the interactions at M^{pro} activation/dimerization site as given in Fig. 4. This was possible for flavonoid compounds and M^{pro}, as their large number of interactions provided ample data to interpret. The molecular weight, rotatable bonds and TPSA values of different categories of flavonoids may be similar and hence activity can be related to hydrogen bond donors and acceptors. The number and position of hydroxyl groups especially at 3, 3' and 7 positions (Anusuya and Gromiha, 2019) are significant in explaining the SARs of flavonoids and are marked in Fig. 7.

The study includes flavonoids from seven subcategories. The flavones luteolin, apigenin, tangeritin are showing 3, 2, and 1 each respectively with the binding energy of −8.9 kcal/mol for both luteolin and apigenin. The lower binding energy and higher interactions (3

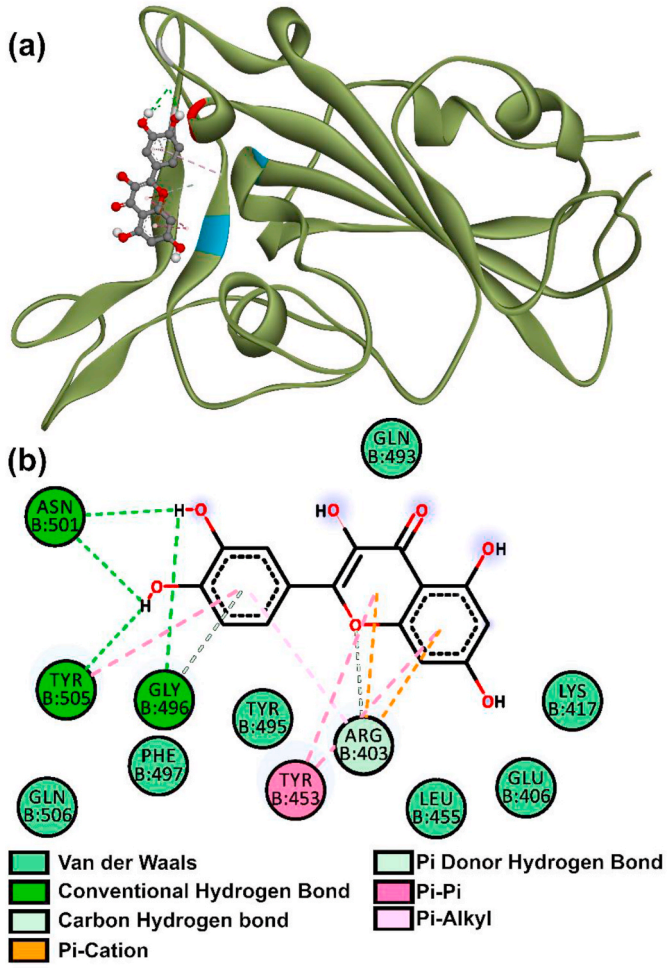

Fig. 6. Binding mode of spike protein and Quercetin in (a) 3D (b) 2D with amino acid interactions.

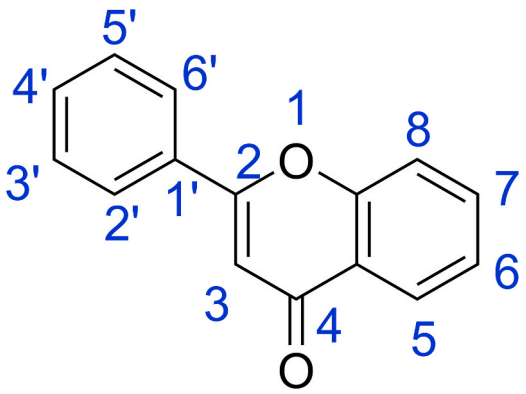

Fig. 7. The general structure of flavonoids.

interactions) of apigenin and luteolin can be assigned to the existence of a hydroxy group at the 7th position of the basic flavonoid structure. The four bulky methoxy groups in tangeritin, however, reduces its interaction to only one protein and also contributes to the higher binding energy of −7.7 kcal/mol. The flavonols category had quercetin, myricetin, kaempferol and fisetin. Here, quercetin and myricetin show interactions with Glu288, Asp289 and Glu290 because of five hydroxyl groups with three –OH groups at 3, 3′ and 7 positions. Kaempferol has four hydroxyl groups with only 2 interactions with Glu288 and Asp289, owing to the absence of –OH at 3' position. However, fisetin with four hydroxyl groups interacts with only one amino acid and has the highest binding energy of −8.7 kcal/mol. Flavones lack an additional –OH group at 3rd position, structurally discriminating them from flavonols and making them less active which is evident from the higher binding energies for same amino acid interactions.

In the case of flavanones, namely, hesperitin, naringenin, eriodictyol and liquiritin, even with the presence of 7 –OH groups, eriodictyol is not interacting with any key residues. The three key interactions of hesperitin can be attributed to the four free hydroxyl groups with three hydroxyl groups in 3, 3' and 7 positions. The number of hydroxyl groups in naringenin is limited to three, with only two in favourable positions and thereby decreasing the number of amino acid interactions to two. However, the presence of beta-D-glucopyranosyl residue at 2nd position and the presence of only one hydroxyl group reduces the interactions of liquiritin to one interaction with Asp289. The result of interaction with isoflavanones was surprising, as daidzein shows interactions with three key amino acids, Glu288, Asp289 and Glu290; while genistein only interacts with Asp289, even though both have only one favourable hydroxyl group at the 7th position. The anthocyanins are structurally similar to flavonols, with the notable absence of C═O in 4th position. Extending the same criteria to anthocyanins, cyanidin and peonidin show three interactions each, and, pelargonidin shows only one amino acid interaction. The lower binding energy of cyanidin (−8.7 kcal/mol) may be due to the presence of five free hydroxyl groups while peonidin (−8.4 kcal/mol) has four free hydroxyl and one methoxy groups.Moving on to chalcones, phloridzin with three hydroxyl groups and one glucoside ring showed three key interactions, followed by chalconaringenin with two key interactions. The indole chalcones were mainly limited to two key interactions. Out of 7 indole chalcones interacting with Glu288 and Asp289, five were heterocyclic compounds. The compound C9, with 3-NH_2 groups capable of H-bonding, also interacted with the aforementioned amino acids. Three indole chalcones, C3, C6 and C16 only interacted with Asp289. The reason for the lower interaction of indole chalcones when compared to flavonoids can be due to the absence of free hydroxyl groups. In a nutshell, the presence of hydroxy groups is favoring the interactions with key residues, while the position and number of hydrogen bonds are important in analyzing the inhibitory potential. The flavonoids and indole chalcones can be plausible agents against SARS-CoV-2 inhibition and the *in vitro* studies should be

implemented to understand their anti- SARS-CoV-2 properties.

5. Conclusion

Natural flavonoids and synthetic indole-chalcones were tested *in silico* for their pharmacokinetic properties and were validated as having druglike nature. This library was considered for tackling the modern-day issue of SARS-CoV-2 and further tested against homology modelled M^{pro}, rdrp and S proteins. Analysis of protein-ligand docking revealed the following: Cyanidin may suppress rdrp by binding at Asp761 catalytic residue, halting the viral replication process. Compounds C25, Daidzein, Eriodictyol, Fisetin, Genistein, Kaempferol, Myricetin, Quercetin, Arbutin, Chalconaringenin, Phloretin and Liquiritin interact on the spike proteins' key RBD and may inhibit spread to receptors limiting viral spread. The most encouraging result was that of M^{pro} with a staggering 30 compounds capable of disrupting activation/dimerization of the protease. A whopping 40 compounds could lower the efficiency of M^{pro} by action at regulatory residues. The indole-chalcones and flavonoids displayed the capability to suppress SARS-CoV-2 proteins and justify their further *in vitro in vivo* studies. Quercetin is an established anti-viral agent for dengue and influenza. It displayed strong interactions on SARS-CoV-2 proteins such as M^{pro} at Glu290 and Asp289, as well as on receptor binding domain of the viral spike based on the computational analysis. These results echo the works on Quercetin by other researchers. Hence, Quercetin is an exceptional candidate for further *in vitro/in vivo* studies.

Author contribution

Balaji Gowrivel Vijayakumar: Design of Study, In silico studies, Data interpretation, Writing - original draft. Deepthi Ramesh: Design of Study, Biology related to SARS-CoV-2, Data interpretation, Writing - original draft. Annu Joji: Pharmacokinetic studies of indole-chalcones, Jayadharini Jayachandra prakasan: Pharmacokinetic studies of Flavonoid, Tharanikkarasu Kannan: Conceptualization, Writing - review & editing, Supervision, Project administration, Funding acquisition

Funding sources

Balaji Gowrivel Vijayakumar thanks Pondicherry University for University Research Fellowship (URF). Deepthi Ramesh thanks DST, New Delhi, India for DST -INSPIRE fellowship (JRF), (No. DST/INSPIRE Fellowship/IF170273 dated January 5 2018). Authors thank University Grants Commission (UGC), New Delhi, India for their financial support under Special Assistance Program, stage DSA-I to Department of Chemistry, Pondicherry University (No. F.540/6/DSA-1/2016/(SAP-1) dated 31-10-2018).

Declaration of competing interest

The authors declared no conflict of interests.

Acknowledgements

Balaji Gowrivel Vijayakumar thanks Pondicherry University for University Research Fellowship (URF), Deepthi Ramesh thanks DST, New Delhi, India for DST INSPIRE Fellowship (JRF) (No. DST/INSPIRE Fellowship/IF170273 dated 5 January 2018) and authors thank University Grants Commission (UGC), New Delhi, India through Special Assistance Program, stage DSA-I for financial assistance to Department of Chemistry, Pondicherry University (No. F.540/6/DSA-1/2016/(SAP-1) dated 31-10-2018).

Appendix A. Supplementary data

Supplementary data to this article can be found online at https://doi.org/10.1016/j.ejphar.2020.173448.

References

AL-Ishaq, R.K., Abotaleb, M., Kubatka, P., Kajo, K., Büsselberg, D., 2019. Flavonoids and their anti-diabetic effects: cellular mechanisms and effects to improve blood sugar levels. Biomolecules 9, 430. https://doi.org/10.3390/biom9090430.

Anand, K., Ziebuhr, J., Wadhwani, P., Mesters, J.R., Hilgenfeld, R., 2003. Coronavirus main proteinase (3CLpro) structure: basis for design of anti-SARS drugs. Science 300, 1763–1767. https://doi.org/10.1126/science.1085658.

Andres, A., Donovan, S.M., Kuhlenschmidt, M.S., 2009. Soy isoflavones and virus infections. J. Nutr. Biochem. 20, 563–569. https://doi.org/10.1016/j.jnutbio.2009.04.004.

Anusuya, S., Gromiha, M.M., 2019. Structural basis of flavonoids as dengue polymerase inhibitors: insights from QSAR and docking studies. J. Biomol. Struct. Dyn. 37, 104–115. https://doi.org/10.1080/07391102.2017.1419146.

Arabyan, E., Hakobyan, A., Kotsinyan, A., Karalyan, Z., Arakelov, V., Arakelov, G., Nazaryan, K., Simonyan, A., Aroutiounian, R., Ferreira, F., Zakaryan, H., 2018. Genistein inhibits African swine fever virus replication in vitro by disrupting viral DNA synthesis. Antivir. Res. 156, 128–137. https://doi.org/10.1016/j.antiviral.2018.06.014.

Argenta, D.F., Silva, I.T., Bassani, V.L., Koester, L.S., Teixeira, H.F., Simões, C.M.O., 2015. Antiherpes evaluation of soybean isoflavonoids. Arch. Virol. 160, 2335–2342. https://doi.org/10.1007/s00705-015-2514-z.

Ashour, H.M., Elkhatib, W.F., Rahman, M.M., Elshabrawy, H.A., 2020. Insights into the recent 2019 novel coronavirus (SARS-CoV-2) in light of past human coronavirus outbreaks. Pathogens 9, 186. https://doi.org/10.3390/pathogens9030186.

Baig, A.M., Khaleeq, A., Ali, U., Syeda, H., 2020. Evidence of the COVID-19 virus targeting the CNS: tissue distribution, host–virus interaction, and proposed neurotropic mechanisms. ACS Chem. Neurosci. 11, 995–998. https://doi.org/10.1021/acschemneuro.0c00122.

Biradar, J.S., Sasidhar, B.S., Parveen, R., 2010. Synthesis, antioxidant and DNA cleavage activities of novel indole derivatives. Eur. J. Med. Chem. 45, 4074–4078. https://doi.org/10.1016/j.ejmech.2010.05.067.

Burmaoglu, S., Algul, O., Gobek, A., Aktas Anil, D., Ulger, M., Erturk, B.G., Kaplan, E., Dogen, A., Aslan, G., 2017. Design of potent fluoro-substituted chalcones as antimicrobial agents. J. Enzym. Inhib. Med. Chem. 32, 490–495. https://doi.org/10.1080/14756366.2016.1265517.

Chahar, M.K., Sharma, N., Dobhal, M.P., Joshi, Y.C., 2011. Flavonoids: a versatile source of anticancer drugs. Pharm. Rev. 5, 1–12. https://doi.org/10.4103/0973-7847.79093.

Chiaradia, L.D., Martins, P.G.A., Cordeiro, M.N.S., Guido, R.V.C., Ecco, G., Andricopulo, A.D., Yunes, R.A., Vernal, J., Nunes, R.J., Terenzi, H., 2012. Synthesis, biological evaluation, and molecular modeling of chalcone derivatives as potent inhibitors of Mycobacterium tuberculosis protein tyrosine phosphatases (PtpA and PtpB). J. Med. Chem. 55, 390–402. https://doi.org/10.1021/jm2012062.

Chirumbolo, S., 2016. Commentary: the antiviral and antimicrobial activities of licorice, a widely-used Chinese herb. Front. Microbiol. 7 https://doi.org/10.3389/fmicb.2016.00531, 531-531.

Cui, J., Li, F., Shi, Z.-L., 2019. Origin and evolution of pathogenic coronaviruses. Nat. Rev. Microbiol. 17, 181–192. https://doi.org/10.1038/s41579-018-0118-9.

Cushnie, T.P.T., Lamb, A.J., 2005. Antimicrobial activity of flavonoids. Int. J. Antimicrob. Agents 26, 343–356. https://doi.org/10.1016/j.ijantimicag.2005.09.002.

Dai, W., Bi, J., Li, F., Wang, S., Huang, X., Meng, X., Sun, B., Wang, D., Kong, W., Jiang, C., Su, W., 2019. Antiviral efficacy of flavonoids against enterovirus 71 infection in vitro and in newborn mice. Viruses 11, 625. https://doi.org/10.3390/v11070625.

Dallakyan, S., Olson, A.J., 2015. Small-molecule library screening by docking with PyRx. Methods Mol. Biol. 1263, 243–250. https://doi.org/10.1007/978-1-4939-2269-7_19.

de Mello, M.V.P., Abrahim-Vieira, B.d.A., Domingos, T.F.S., de Jesus, J.B., de Sousa, A.C.C., Rodrigues, C.R., Souza, A.M.T.d., 2018. A comprehensive review of chalcone derivatives as antileishmanial agents. Eur. J. Med. Chem. 150, 920–929. https://doi.org/10.1016/j.ejmech.2018.03.047.

Dong, W., Wei, X., Zhang, F., Hao, J., Huang, F., Zhang, C., Liang, W., 2014. A dual character of flavonoids in influenza A virus replication and spread through modulating cell-autonomous immunity by MAPK signaling pathways. Sci. Rep. 4, 7237. https://doi.org/10.1038/srep07237.

Elfiky, A.A., 2020. Ribavirin, remdesivir, sofosbuvir, galidesivir, and tenofovir against SARS-CoV-2 RNA dependent RNA polymerase (RdRp): a molecular docking study. Life Sci. 253, 117592. https://doi.org/10.1016/j.lfs.2020.117592.

Fan, W., Qian, S., Qian, P., Li, X., 2016. Antiviral activity of luteolin against Japanese encephalitis virus. Virus Res. 220, 112–116. https://doi.org/10.1016/j.virusres.2016.04.021.

Frabasile, S., Koishi, A.C., Kuczera, D., Silveira, G.F., Verri Jr., W.A., Duarte Dos Santos, C.N., Bordignon, J., 2017. The citrus flavanone naringenin impairs dengue virus replication in human cells. Sci. Rep. 7 https://doi.org/10.1038/srep41864, 41864-41864.

Gao, Y., Yan, L., Huang, Y., Liu, F., Zhao, Y., Cao, L., Wang, T., Sun, Q., Ming, Z., Zhang, L., Ge, J., Zheng, L., Zhang, Y., Wang, H., Zhu, Y., Zhu, C., Hu, T., Hua, T., Zhang, B., Yang, X., Li, J., Yang, H., Liu, Z., Xu, W., Guddat, L.W., Wang, Q., Lou, Z., Rao, Z., 2020. Structure of the RNA-dependent RNA polymerase from COVID-19 virus. Science. https://doi.org/10.1126/science.abb7498.

Guo, Y.-R., Cao, Q.-D., Hong, Z.-S., Tan, Y.-Y., Chen, S.-D., Jin, H.-J., Tan, K.-S., Wang, D.-Y., Yan, Y., 2020. The origin, transmission and clinical therapies on coronavirus disease 2019 (COVID-19) outbreak – an update on the status. Mil. Med. Res. 7, 11. https://doi.org/10.1186/s40779-020-00240-0.

Gupte, A., Buolamwini, J.K., 2009. Synthesis and biological evaluation of phloridzin analogs as human concentrative nucleoside transporter 3 (hCNT3) inhibitors. Bioorg. Med. Chem. Lett 19, 917–921. https://doi.org/10.1016/j.bmcl.2008.11.112.

Hassan, S.T.S., Masarčíková, R., Berchová, K., 2015. Bioactive natural products with anti-herpes simplex virus properties, 67, pp. 1325–1336. https://doi.org/10.1111/jphp.12436.

He, J.-W., Yang, L., Mu, Z.-q., Zhu, Y.-Y., Zhong, G.-Y., Liu, Z.-Y., Zhou, Q.-G., Cheng, F., 2018. Anti-inflammatory and antioxidant activities of flavonoids from the flowers of Hosta plantaginea. RSC Adv. 8, 18175–18179. https://doi.org/10.1039/C8RA00443A.

Jacome, R., Becerra, A., Ponce de Leon, S., Lazcano, A., 2015. Structural analysis of monomeric RNA-dependent polymerases: evolutionary and therapeutic implications. PloS One 10, e0139001. https://doi.org/10.1371/journal.pone.0139001.

Jin, Z., Du, X., Xu, Y., Deng, Y., Liu, M., Zhao, Y., Zhang, B., Li, X., Zhang, L., Peng, C., Duan, Y., Yu, J., Wang, L., Yang, K., Liu, F., Jiang, R., Yang, X., You, T., Liu, X., Yang, X., Bai, F., Liu, H., Liu, X., Guddat, L.W., Xu, W., Xiao, G., Qin, C., Shi, Z., Jiang, H., Rao, Z., Yang, H., 2020a. Structure of M(pro) from SARS-CoV-2 and discovery of its inhibitors. Nature. https://doi.org/10.1038/s41586-020-2223-y.

Jin, Z., Du, X., Xu, Y., Deng, Y., Liu, M., Zhao, Y., Zhang, B., Li, X., Zhang, L., Peng, C., Duan, Y., Yu, J., Wang, L., Yang, K., Liu, F., Jiang, R., Yang, X., You, T., Liu, X., Yang, X., Bai, F., Liu, H., Liu, X., Guddat, L.W., Xu, W., Xiao, G., Qin, C., Shi, Z., Jiang, H., Rao, Z., Yang, H., 2020b. Structure of Mpro from COVID-19 virus and discovery of its inhibitors. Nature. https://doi.org/10.1038/s41586-020-2223-y.

Kannan, S., Kolandaivel, P., 2018. The inhibitory performance of flavonoid cyanidin-3-sambubiocide against H274Y mutation in H1N1 influenza virus. J. Biomol. Struct. Dyn. 36, 4255–4269. https://doi.org/10.1080/07391102.2017.1413422.

Kaur, R., Sharma, P., Gupta, G.K., Ntie-Kang, F., Kumar, D., 2020. Structure-activity-relationship and mechanistic insights for anti-HIV natural products, 25, p. 2070. https://doi.org/10.3390/molecules25092070.

Kiat, T.S., Pippen, R., Yusof, R., Ibrahim, H., Khalid, N., Rahman, N.A., 2006. Inhibitory activity of cyclohexenyl chalcone derivatives and flavonoids of fingerroot, Boesenbergia rotunda (L.), towards dengue-2 virus NS3 protease. Bioorg. Med. Chem. Lett 16, 3337–3340. https://doi.org/10.1016/j.bmcl.2005.12.075.

Lalani, S., Poh, C.L., 2020. Flavonoids as Antiviral Agents for Enterovirus A71, 184 (EV-A71). 12.

Laskowski, R., Macarthur, M.W., Moss, D.S., Thornton, J., 1993. PROCHECK: a program to check the stereochemical quality of protein structures. J. Appl. Crystallogr. 26, 283–291. https://doi.org/10.1107/S0021889892009944.

LeCher, J.C., Diep, N., Krug, P.W., Hilliard, J.K., 2019. Genistein has antiviral activity against herpes B virus and acts synergistically with antiviral treatments to reduce effective dose. Viruses 11, 499. https://doi.org/10.3390/v11060499.

Lee, J.S., Bukhari, S.N.A., Fauzi, N.M., 2015. Effects of chalcone derivatives on players of the immune system. Drug Des. Dev. Ther. 9, 4761–4778. https://doi.org/10.2147/DDDT.S86242.

Li, T., Zhuang, S., Wang, Y., Wang, Y., Wang, W., Zhang, H., Chen, L., Wang, D., Zhou, Z., Yang, W., 2016. Flavonoid profiling of a traditional Chinese medicine formula of Huangqin Tang using high performance liquid chromatography. Acta Pharm. Sin. B 6, 148–157. https://doi.org/10.1016/j.apsb.2016.01.001.

Lin, Y.-J., Chang, Y.-C., Hsiao, N.-W., Hsieh, J.-L., Wang, C.-Y., Kung, S.-H., Tsai, F.-J., Lan, Y.-C., Lin, C.-W., 2012. Fisetin and rutin as 3C protease inhibitors of enterovirus A71. J. Virol Methods 182, 93–98. https://doi.org/10.1016/j.jviromet.2012.03.020.

Lin, S.-C., Chen, M.-C., Liu, S., Callahan, V.M., Bracci, N.R., Lehman, C.W., Dahal, B., de la Fuente, C.L., Lin, C.-C., Wang, T.T., Kehn-Hall, K., 2019. Phloretin inhibits Zika virus infection by interfering with cellular glucose utilisation. Int. J. Antimicrob. Agents 54, 80–84. https://doi.org/10.1016/j.ijantimicag.2019.03.017.

Lipinski, C.A., Lombardo, F., Dominy, B.W., Feeney, P.J., 1997. Experimental and computational approaches to estimate solubility and permeability in drug discovery and development settings. Adv. Drug Deliv. Rev. 23, 3–25. https://doi.org/10.1016/S0169-409X(96)00423-1.

Liu, W.-H., Liu, Y.-W., Chen, Z.-F., Chiou, W.-F., Tsai, Y.-C., Chen, C.-C., 2015. Calophyllolide content in Calophyllum inophyllum at different stages of maturity and its osteogenic activity, 20, pp. 12314–12327. https://doi.org/10.3390/molecules200712314.

Lovell, S.C., Davis, I.W., Arendall III, W.B., de Bakker, P.I.W., Word, J.M., Prisant, M.G., Richardson, J.S., Richardson, D.C., 2003. Structure validation by Cα geometry: φ,ψ and Cβ deviation. Proteins 50, 437–450. https://doi.org/10.1002/prot.10286.

Migas, P., Krauze-Baranowska, M., 2015. The significance of arbutin and its derivatives in therapy and cosmetics. Phytochemistry Letters 13. https://doi.org/10.1016/j.phytol.2015.05.015.

Mohammadi Pour, P., Fakhri, S., Asgary, S., Farzaei, M.H., Echeverría, J., 2019. The signaling pathways, and therapeutic targets of antiviral agents: focusing on the antiviral approaches and clinical perspectives of anthocyanins in the management of viral diseases. Front. Pharmacol. 10 https://doi.org/10.3389/fphar.2019.01207, 1207-1207.

Molinspiration cheminformatics. http://www.molinspiration.com, 2002.

Neuman, B.W., Kiss, G., Kunding, A.H., Bhella, D., Baksh, M.F., Connelly, S., Droese, B., Klaus, J.P., Makino, S., Sawicki, S.G., Siddell, S.G., Stamou, D.G., Wilson, I.A., Kuhn, P., Buchmeier, M.J., 2011. A structural analysis of M protein in coronavirus assembly and morphology. J. Struct. Biol. 174, 11–22. https://doi.org/10.1016/j.jsb.2010.11.021.

Park, J.-Y., Ko, J.-A., Kim, D.W., Kim, Y.M., Kwon, H.-J., Jeong, H.J., Kim, C.Y., Park, K. H., Lee, W.S., Ryu, Y.B., 2016. Chalcones isolated from Angelica keiskei inhibit cysteine proteases of SARS-CoV. J. Enzym. Inhib. Med. Chem. 31, 23–30. https://doi.org/10.3109/14756366.2014.1003215.

Pires, D.E.V., Blundell, T.L., Ascher, D.B., 2015. pkCSM: predicting small-molecule pharmacokinetic and toxicity properties using graph-based signatures. J. Med. Chem. 58, 4066–4072. https://doi.org/10.1021/acs.jmedchem.5b00104.

Polansky, H., Lori, G., 2020. Coronavirus disease 2019 (COVID-19): first indication of efficacy of Gene-Eden-VIR/Novirin in SARS-CoV-2 infection. Int. J. Antimicrob. Agents 105971. https://doi.org/10.1016/j.ijantimicag.2020.105971. -105971.

Qian, S., Fan, W., Qian, P., Zhang, D., Wei, Y., Chen, H., Li, X., 2015. Apigenin restricts FMDV infection and inhibits viral IRES driven translational activity. Viruses 7, 1613–1626. https://doi.org/10.3390/v7041613.

Rahman, N., Basharat, Z., Yousuf, M., Castaldo, G., Rastrelli, L., Khan, H., 2020. Virtual screening of natural products against type II transmembrane serine protease (TMPRSS2), the priming agent of coronavirus 2 (SARS-CoV-2). Molecules 25, 2271. https://doi.org/10.3390/molecules25102271.

Ramesh, D., Joji, A., Vijayakumar, B.G., Sethumadhavan, A., Mani, M., Kannan, T., 2020. Indole chalcones: design, synthesis, in vitro and in silico evaluation against Mycobacterium tuberculosis. Eur. J. Med. Chem. 198, 112358. https://doi.org/10.1016/j.ejmech.2020.112358.

Salehi, B., Fokou, P.V.T., Sharifi-Rad, M., Zucca, P., Pezzani, R., Martins, N., Sharifi-Rad, J., 2019. The therapeutic potential of naringenin: a review of clinical trials. Pharmaceuticals 12, 11. https://doi.org/10.3390/ph12010011.

Schwede, T., Kopp, J., Guex, N., Peitsch, M.C., 2003. SWISS-MODEL: an automated protein homology-modeling server. Nucleic Acids Res. 31, 3381–3385. https://doi.org/10.1093/nar/gkg520.

Semwal, D.K., Semwal, R.B., Combrinck, S., Viljoen, A., 2016. Myricetin: a dietary molecule with diverse biological activities. Nutrients 8. https://doi.org/10.3390/nu8020090, 90-90.

Shi, J., Song, J., 2006. The catalysis of the SARS 3C-like protease is under extensive regulation by its extra domain. FEBS J. 273, 1035–1045. https://doi.org/10.1111/j.1742-4658.2006.05130.x.

Shi, J., Sivaraman, J., Song, J., 2008. Mechanism for controlling the dimer-monomer switch and coupling dimerization to catalysis of the severe acute respiratory syndrome coronavirus 3C-like protease. J. Virol. 82, 4620–4629. https://doi.org/10.1128/JVI.02680-07.

South, A.M., Tomlinson, L., Edmonston, D., Hiremath, S., Sparks, M.A., 2020. Controversies of renin-angiotensin system inhibition during the COVID-19 pandemic. Nat. Rev. Nephrol. https://doi.org/10.1038/s41581-020-0279-4.

Tan, Y.W., Fung, T.S., Shen, H., Huang, M., Liu, D.X., 2018. Coronavirus infectious bronchitis virus non-structural proteins 8 and 12 form stable complex independent of the non-translated regions of viral RNA and other viral proteins. Virology 513, 75–84. https://doi.org/10.1016/j.virol.2017.10.004.

Tang, X., Su, S., Chen, M., He, J., Xia, R., Guo, T., Chen, Y., Zhang, C., Wang, J., Xue, W., 2019. Novel chalcone derivatives containing a 1,2,4-triazine moiety: design, synthesis, antibacterial and antiviral activities. RSC Adv. 9, 6011–6020. https://doi.org/10.1039/C9RA00618D.

Tang, X., Zhang, C., Chen, M., Xue, Y., Liu, T., Xue, W., 2020. Synthesis and antiviral activity of novel myricetin derivatives containing ferulic acid amide scaffolds. New J. Chem. 44, 2374–2379. https://doi.org/10.1039/C9NJ05867B.

Trott, O., Olson, A.J., 2010. AutoDock Vina: improving the speed and accuracy of docking with a new scoring function, efficient optimization, and multithreading. J. Comput. Chem. 31, 455–461. https://doi.org/10.1002/jcc.21334.

Vázquez-Calvo, Á., Jiménez de Oya, N., Martín-Acebes, M.A., Garcia-Moruno, E., Saiz, J.-C., 2017. Antiviral properties of the natural polyphenols Delphinidin and epigallocatechin gallate against the flaviviruses west nile virus, zika virus, and dengue virus. Front. Microbiol. 8 https://doi.org/10.3389/fmicb.2017.01314, 1314-1314.

Veber, D.F., Johnson, S.R., Cheng, H.-Y., Smith, B.R., Ward, K.W., Kopple, K.D., 2002. Molecular properties that influence the oral bioavailability of drug candidates. J. Med. Chem. 45, 2615–2623. https://doi.org/10.1021/jm020017n.

Venkataraman, S., Prasad, B.V.L.S., Selvarajan, R., 2018. RNA dependent RNA polymerases: insights from structure, function and evolution. Viruses 10, 76. https://doi.org/10.3390/v10020076.

Wang, Q., Wong, G., Lu, G., Yan, J., Gao, G.F., 2016. MERS-CoV spike protein: targets for vaccines and therapeutics. Antivir. Res. 133, 165–177. https://doi.org/10.1016/j.antiviral.2016.07.015.

Wang, Y., Chen, Y., Chen, Y., Zhou, B., Shan, X., Yang, G., 2018. Eriodictyol inhibits IL-1β-induced inflammatory response in human osteoarthritis chondrocytes. Biomed. Pharmacother. 107, 1128–1134. https://doi.org/10.1016/j.biopha.2018.08.103.

Wang, Q., Zhang, Y., Wu, L., Niu, S., Song, C., Zhang, Z., Lu, G., Qiao, C., Hu, Y., Yuen, K. Y., Wang, Q., Zhou, H., Yan, J., Qi, J., 2020. Structural and functional basis of SARS-CoV-2 entry by using human ACE2. Cell. https://doi.org/10.1016/j.cell.2020.03.045.

Wei, P., Fan, K., Chen, H., Ma, L., Huang, C., Tan, L., Xi, D., Li, C., Liu, Y., Cao, A., Lai, L., 2006. The N-terminal octapeptide acts as a dimerization inhibitor of SARS coronavirus 3C-like proteinase. Biochem. Biophys. Res. Commun. 339, 865–872. https://doi.org/10.1016/j.bbrc.2005.11.102.

Weidenbörner, M., Hindorf, H., Jha, H.C., Tsotsonos, P., 1990. Antifungal activity of flavonoids against storage fungi of the genus Aspergillus. Phytochemistry 29, 1103–1105. https://doi.org/10.1016/0031-9422(90)85412-9.

Weiss, S.R., Leibowitz, J.L., 2011. Coronavirus pathogenesis. Adv. Virus Res. 81, 85–164. https://doi.org/10.1016/B978-0-12-385885-6.00009-2.

Wu, J.-H., Wang, X.-H., Yi, Y.-H., Lee, K.-H., 2003. Anti-AIDS agents 54. A potent anti-HIV chalcone and flavonoids from genus Desmos. Bioorg. Med. Chem. Lett 13, 1813–1815. https://doi.org/10.1016/S0960-894X(03)00197-5.

Wu, W., Li, R., Li, X., He, J., Jiang, S., Liu, S., Yang, J., 2015. Quercetin as an antiviral agent inhibits influenza A virus (iav) entry. Viruses 8, 6. https://doi.org/10.3390/v8010006.

Wu, C., Liu, Y., Yang, Y., Zhang, P., Zhong, W., Wang, Y., Wang, Q., Xu, Y., Li, M., Li, X., Zheng, M., Chen, L., Li, H., 2020a. Analysis of therapeutic targets for SARS-CoV-2 and discovery of potential drugs by computational methods. Acta Pharm. Sin. B. https://doi.org/10.1016/j.apsb.2020.02.008.

Wu, F., Zhao, S., Yu, B., Chen, Y.-M., Wang, W., Song, Z.-G., Hu, Y., Tao, Z.-W., Tian, J.-H., Pei, Y.-Y., Yuan, M.-L., Zhang, Y.-L., Dai, F.-H., Liu, Y., Wang, Q.-M., Zheng, J.-J., Xu, L., Holmes, E.C., Zhang, Y.-Z., 2020b. A new coronavirus associated with human respiratory disease in China. Nature 579, 265–269. https://doi.org/10.1038/s41586-020-2008-3.

Xu, S.L., Zhu, K.Y., Bi, C.W.C., Yan, L., Men, S.W.X., Dong, T.T.X., Tsim, K.W.K., 2013. Flavonoids, derived from traditional Chinese medicines, show roles in the differentiation of neurons: possible targets in developing health food products. Birth Defect Res C 99, 292–299. https://doi.org/10.1002/bdrc.21054.

Xu, J.-J., Wu, X., Li, M.-M., Li, G.-Q., Yang, Y.-T., Luo, H.-J., Huang, W.-H., Chung, H.Y., Ye, W.-C., Wang, G.-C., Li, Y.-L., 2014. Antiviral activity of polymethoxylated flavones from "guangchenpi", the edible and medicinal pericarps of citrus reticulata 'chachi'. J. Agric. Food Chem. 62, 2182–2189. https://doi.org/10.1021/jf404310y.

Yang, H., Yang, M., Ding, Y., Liu, Y., Lou, Z., Zhou, Z., Sun, L., Mo, L., Ye, S., Pang, H., Gao, G.F., Anand, K., Bartlam, M., Hilgenfeld, R., Rao, Z., 2003. The crystal structures of severe acute respiratory syndrome virus main protease and its complex with an inhibitor. Proc. Natl. Acad. Sci. U. S. A. 100, 13190–13195. https://doi.org/10.1073/pnas.1835675100.

Yin, W., Mao, C., Luan, X., Shen, D.D., Shen, Q., Su, H., Wang, X., Zhou, F., Zhao, W., Gao, M., Chang, S., Xie, Y.C., Tian, G., Jiang, H.W., Tao, S.C., Shen, J., Jiang, Y., Jiang, H., Xu, Y., Zhang, S., Zhang, Y., Xu, H.E., 2020. Structural basis for inhibition of the RNA-dependent RNA polymerase from SARS-CoV-2 by remdesivir. Science. https://doi.org/10.1126/science.abc1560.

Yixi, X., Weijie, Y., Fen, T., Xiaoqing, C., Licheng, R., 2015. Antibacterial activities of flavonoids: structure-activity relationship and mechanism. Curr. Med. Chem. 22, 132–149. https://doi.org/10.2174/0929867321666140916113443.

Yu, J.-Y., Ha, J.Y., Kim, K.-M., Jung, Y.-S., Jung, J.-C., Oh, S., 2015. Anti-Inflammatory activities of licorice extract and its active compounds, glycyrrhizic acid, liquiritin and liquiritigenin. In: BV2 Cells and Mice Liver. Molecules (Basel, Switzerland), vol. 20, pp. 13041–13054. https://doi.org/10.3390/molecules200713041.

Zandi, K., Teoh, B.-T., Sam, S.-S., Wong, P.-F., Mustafa, M.R., AbuBakar, S., 2011. Antiviral activity of four types of bioflavonoid against dengue virus type-2. Virol. J. 8, 560. https://doi.org/10.1186/1743-422X-8-560.

Zhang, W.-Y., Lee, J.-J., Kim, Y., Kim, I.-S., Han, J.-H., Lee, S.-G., Ahn, M.-J., Jung, S.-H., Myung, C.-S., 2012. Effect of eriodictyol on glucose uptake and insulin resistance in vitro. J. Agric. Food Chem. 60, 7652–7658. https://doi.org/10.1021/jf300601z.

Zhang, W., Qiao, H., Lv, Y., Wang, J., Chen, X., Hou, Y., Tan, R., Li, E., 2014. Apigenin inhibits enterovirus-71 infection by disrupting viral RNA association with trans-acting factors. PloS One 9, e110429. https://doi.org/10.1371/journal.pone.0110429.

Zhang, H., Penninger, J.M., Li, Y., Zhong, N., Slutsky, A.S., 2020a. Angiotensin-converting enzyme 2 (ACE2) as a SARS-CoV-2 receptor: molecular mechanisms and potential therapeutic target. Intensive Care Med. 46, 586–590. https://doi.org/10.1007/s00134-020-05985-9.

Zhang, L., Lin, D., Sun, X., Curth, U., Drosten, C., Sauerhering, L., Becker, S., Rox, K., Hilgenfeld, R., 2020b. Crystal structure of SARS-CoV-2 main protease provides a basis for design of improved alpha-ketoamide inhibitors. Science 368, 409–412. https://doi.org/10.1126/science.abb3405.

Zhou, P., Yang, X.-L., Wang, X.-G., Hu, B., Zhang, L., Zhang, W., Si, H.-R., Zhu, Y., Li, B., Huang, C.-L., Chen, H.-D., Chen, J., Luo, Y., Guo, H., Jiang, R.-D., Liu, M.-Q., Chen, Y., Shen, X.-R., Wang, X., Zheng, X.-S., Zhao, K., Chen, Q.-J., Deng, F., Liu, L.-L., Yan, B., Zhan, F.-X., Wang, Y.-Y., Xiao, G.-F., Shi, Z.-L., 2020. A pneumonia outbreak associated with a new coronavirus of probable bat origin. Nature 579, 270–273. https://doi.org/10.1038/s41586-020-2012-7.